High-performance Electrical Variable Resistor Sensor for E.coli O157:H7 Detection

R. D. A. A. Rajapaksha[1], U. Hashim[1, 2], M. N. Afnan Uda[2] and C. A. N. Fernando[3]

[1]*Institute of Nano Electronic Engineering, Universiti Malaysia Perlis, 01000 Kangar, Perlis, Malaysia.*
[2]*School of Microelectronic Electronic Engineering, Universiti Malaysia Perlis, 01000 Kangar, Perlis, Malaysia.*
[3]*Nano Technology Research Laboratory, Department of Electronics, Faculty of Applied Sciences, Wayamba University of Sri Lanka, Kuliyapitiya, Sri Lanka.*
uda@unimap.edu.my

Abstract— **Nowadays interdigitated electrode (IDE) based sensors have stimulated increasing interest in the application of biosensor field. A large number of finger electrodes as comb structure gain high sensitivity through electrical measurements. In this research study, we have demonstrated a novel mechanism as biocontrollable variable resistor through solid state conducting Polymer Bridge to detect single-stranded E. coliO157:H7 DNA. The gap of AuIDE sensor on Si substrate was used to create DNA biosensor. Functionalization steps of the AuIDE to create biosensor was based on silanization by APTES, immobilization of E.coli O157:H7 synthetic probe single-stranded DNA (ssDNA), blocking with tween-20. The well fabricated AuIDE biosensor was physically characterized by using scanning electron microscope (SEM) and high power microscope (HPM). Molecular assembly of the functionalized biosensor was analyzed structurally using Energy-dispersive X-ray spectroscopy (EDX) and electrically using current–voltage measurements (I-V). The selectivity of the biosensor was identified electrically using complementary, non-complementary and single base mismatch ssDNA targets. Blocking step with tween-20 was important to detect target specifically. The obtained variations in current indicate the varied concentrations of E. coli targets and it is confirmed that biosensor is suitable to detect different concentrations in the range from 10 fM to 10 µM.**

Index Terms—**DNA Sensor; E.coli O157:H7; Hybridization; Interdigitated Electrode; Variable Resister Sensor.**

I. INTRODUCTION

Escherichia coli (*E. coli*) O157:H7 is one of the most serious food pathogenic bacterial species mentioned as pathotypes. Its infection leads to watery diarrhea associated with a number of pathological symptoms, such as vomiting, fever and dehydration [1-2]. The *E. coli* pathology causes watery diarrhea with the presence of abdominal cramps but no fever and it does not show the invasion of blood vessels, but is characterized by persistent skin rashes and chronic watery diarrhea. So that, generation of the right sensing strategy for *E.coli O157:H7* will pave the way for easier detection and curing.

Conventional methods of detecting foodborne pathogen causing diseases have limitations such as low sensitivity, typically in the sub-millimolar range. However, only in special cases the sensitivity could reach the femtomolar range [3-6].

To overcome the drawbacks of the conventional methods as above mentioned, the commercial application of biosensor shows a significant impact in the fields of medical diagnostics and food analysis. Nowadays, biosensor researchers are widely concentrated, numerous research and excellent reviews have been published [7-9]. It is mainly due to the reason that biosensors have imposed to be a powerful analytical tool that produces higher sensitivity, specificity, repeatability and real-time in-field detection [10-15].

Current work is focused on the concept of a DNA biosensor able to detect the presence of specific target single-stranded DNA (ssDNA) sequences from *E.coli O157:H7*. The AuIDE surface was functionalized until probe *E.coli O157:H7* ssDNA and tween-20 was used as the blocking agent to prepare biosensor for specific *E.coli O157:H7* ssDNA target detection. The functionalized biosensor was morphologically characterized using scanning electron microscope (SEM), and high power microscope (HPM), structural analysis was done using Energy-dispersive X-ray spectroscopy (EDX) and Current-Voltage (I-V) characteristics were used to reveal the specificity of the target and to detect different concentrations.

II. MATERIALS AND METHODS

A. Chemicals, Reagents and Oligonucleotides

All 30-mer oligonucleotides ssDNA specific to *E.coli O157:H7*were purchased from AIT Biotech, Singapore and *E.coli O157:H7* nucleotide gene sequence used to design the probe in this study was collected from GenBank database. The respective oligonucleotides and sequences are presented in Table 1. As shown above 5' end of binding *E.coli O157:H7* ssDNA probe was terminated with a carboxyl group. APTES [(3-Aminopropyl) triethoxysilane:NH2-(CH2)3-Si(OC2H5)3] was obtained from Sigma-Aldrich, the USA, used for silanization and tween-20 was used as blocking agent. Other required chemicals like acetone and ethanol were in analytical reagent grade and purchased commercially. Deionized distilled water (DDI-water) was used throughout this experiment.

Table 1
30-mer DNA Sequences for *E.coli O157:H7*DNA Probe, Complementary, Non-Complementary and Single Base Mismatch.

Oligonucleotide	Sequences
30-mer probe	5'-(COOH) AAC GCC GAT ACC ATT ACT TAT ACC GCG ACG–3'
30-mer complementary	(5'-CGT CGC GGT ATA AGT AAT GGT ATC GGC GTT–3')
30-mer non-complementary	(5'-GCA GCG CCA TAT TCA TTA CCA TAG CCG CAA–3')
30-mer single base mismatch	(5'-CGT CGC GGT ATA ACT AAT GGT ATC GGC GTT–3')

B. Instruments

The surface morphology of the AuIDE pattern was characterized by using high power microscope (HPM) and scanning electron microscope (SEM)(JEOL, JSM- 610LV), which were operated at 20kV with 7000 magnification under the room temperature and the 3D analysis of grain between IDE finger electrodes were characterized by Hawk 3D nano-profiler with 50k magnification. The biosensor functionalization steps were characterized using EDX (OXFORD instrument). Incubation process was done by using Weifo Electronic dry cabinet. The measurements for I-V characteristics were carried out by 2450 Picoammeter/Voltage Source (Keithley 2500) with probe station.

C. Silanization, Immobilization and Hybridization

The active area of the bare AuIDE was washed with NaOH to make hydroxyl layer on the SiO_2 surface. Then, bare AuIDE surface was functionalized with APTES. Carboxyl-modified synthetic ssDNA probes and target oligonucleotides were used specifically for *E.coli O157:H7* for interaction analysis. Stock solutions of all oligonucleotides were re-suspended in autoclaved ultrapure water (>18MΩ) to obtain 10 μM solution and kept -20°C. After modification of the AuIDE transducer with APTES, 1 μl ssDNA probe was immobilized on the transducer surface to form a recognition layer through the covalent amide bond of the APTES with the carboxyl group of ssDNA probe. The transducer surface was rinsed with DI water to remove unbound probe ssDNA. Tween-20 was used to block the non-immobilized surface. The hybridization reaction was performed with the complimentary, non-complementary and mismatch target ssDNA by dropping 1μl to the active surface area in the biosensor. The surface was rinsed with DI water to remove non-hybridized ssDNA targets before taking electrical measurements. Current measurements were carried out for each functionalization step and after the hybridization processes to determine the conductivity changes.

III. RESULTS AND DISCUSSION

A. Physical Characterization Before Functionalization

The physical characterization of the AuIDE surface is displayed in Figure 1. Image (A)shows that HPM image for 45x resolution power and it was confirmed that gap between twin electrodes and a finger width of the IDE are 4μm and 6μm, respectively. The SEM image depicts the sharp and even edges of the IDE fingers as indicated in the image (B) with x7000 magnification. The average finger size of the electrodes is 6μm and average gap size between fingers is 4μm. Sharp edges as shown in figure confirmed that the etching had attained the maximum level in the developed design. EDX spectrum confirms that the materials as silicon (Si), oxygen (O) and Gold (Au) which were included in the bare AuIDE without other material contamination as shown in the image (C). Analysis of the IDE structure with 3D profiler depicts evenly arranged electrode edges, which might further confirm that etching has reached the maximum level of the developmental process [image (D)]. Minimum height of the gold surface form the grain with 6240nm, the maximum height of the surface is 8514 nm and average height is 6910nm, were confirmed by the uniformity of the surface [inset table].
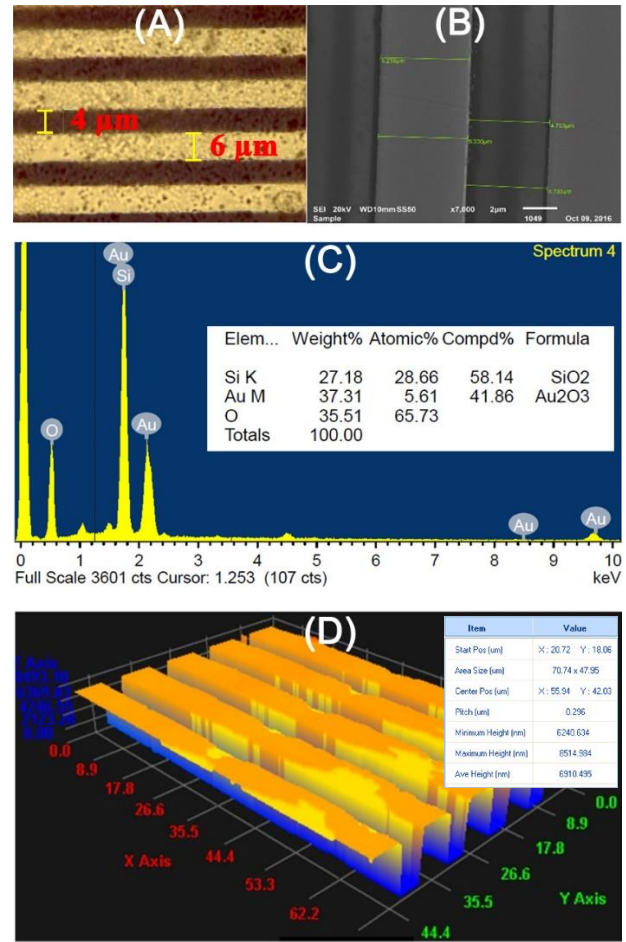

Figure 1: (A) HPM image of the active surface area of the AuIDE for 45x magnifications, (B) SEM image of AuIDE at 7000x magnification, (C) EDX spectrum for AuIDE and (D) shows the 3D profile of the IDE surface and specific parameters

B. Physical Characterization After Functionalization

The surface morphology of the IDE after functionalized with APTES and ssDNA probes can be seen in the SEM image at x600 magnification as shown Figure 2 (A). It is clearly shown that functionalized and non-functionalized area. In here finger gaps cannot be seen because of the low magnification compared to before functionalized SEM image in high magnification at x7000 as shown in Figure 1(B). The Figure 2 (B) is depicted the EDX spectrum after functionalization steps. Additional EDX peaks can be seen for nitrogen, carbon and oxygen as shown in the image (B) compared to Figure 1 (C). These peaks generate due to amine groups in APTES and DNAs.
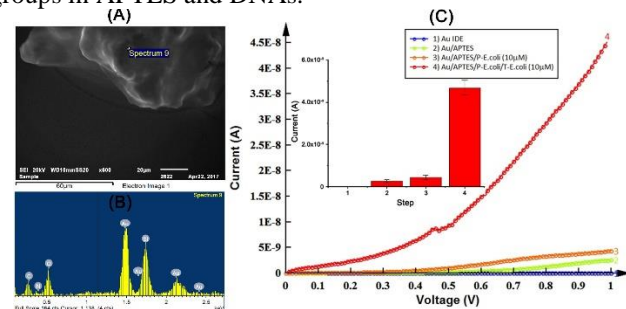

Figure 2: (A) SEM image after functionalization, (B) EDX spectrum after functionalization, (C) I-V characteristics for fabrication steps; (1) bare IDE, (2) silanization with APTES, (3) immobilization with carboxylic probe *E.coli O157:H7* ssDNA probes and (4) shows I-V characteristics after hybridized with complementary *E.coli O157:H7* target ssDNA. The inset graph shows the current for each step at 1V.

Figure 2 (C) shows the I-V characteristics in different steps as functionalization, immobilization and hybridization. In the beginning, AuIDE was electrically characterized by sweeping voltages from 0V to 1V as previous researchers have done in our research group [16]–[18]. Curve 1 shows I-V measurements for the bare AuIDE before functionalization with APTES. The value 23.97 pA current was given at 1V because of the resistance between non shorted fingers. This picoampere low current value verified that the IDE fingers are well fabricated without any short circuit between the main electrodes. According to our best knowledge if IDE fingers shorted, the current varies at milliampere range[7]. Curve 2 shows I-V measurements of IDE after silanization with APTES. After introducing APTES the current was enhanced to 5.08×10^{-9} A at 1 V. This phenomenon occurs due to the protonation ($-H^+$) and deprotonation ($-H^-$) of the amine ($-NH_2$) in APTES and silanol ($-SiOH$) groups on the top of the SiO_2 layer. The current generation mechanism between two fingers can be further explained by using following equations,

$$R = \frac{(\rho L)}{A} \qquad (1)$$

where: R = Resistance of the solid-state polymer layer
ρ =   Resistivity of the solid state polymer layer
L =   Gap between finger electrodes
A =   cross section area of the polymer layer between finger electrodes

$$I = \frac{V}{R} \qquad (2)$$

where: I =   Generated   current   between   finger electrodes
V =   Supply voltage
R =   Resistance of the conducting polymer layer

Curve 3 shows I-V characteristics after immobilization of ssDNA probes on the APTES and it indicates 6.84×10^{-9} A at 1 V. Single strand DNA is negatively charged and it increases the surface charge density in the APTES layer due to the enhancement of the negatively charged ssDNA backbone. After immobilization of ssDNA probes, it makes electrostatic charge between APTES and ssDNA probes. Thus, the resistivity of the polymer medium decreased because of more protons were released from the secondary amine group in APTES and silanol ($-SiOH$) to the polymer medium. Therefore, generated current flow between electrodes was increased due to the enhancement of the proton density.

After hybridization, the resulting current was abruptly increased as shown in I-V characteristic curve 4 and it was shown 4.61×10^{-8} A at 1V. Here *E. coli* ssDNA probe hybridizes with complementary *E. coli* ssDNA target through DNA base pairs and it increases total proton charge density in the APTES.
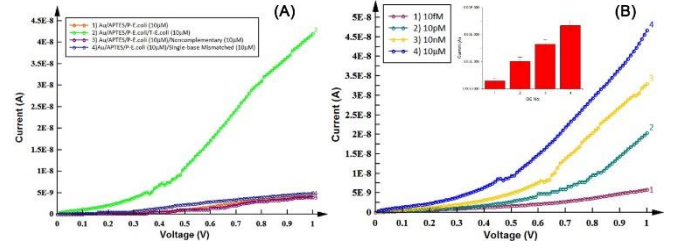

Figure 3: Image (A) - Current responses of different targets as complementary, non-complementary and single base mismatch ssDNAs. Image (B) - Current values for different *E.coli O157:H7* target ssDNA concentrations at 1V.

The I-V characteristics for selectivity measurements were done independently for complementary, non-complementary and single base mismatched *E.coli O157:H7* 30mer ssDNA with 10µM concentration [Figure 3 (A)]. This measurement step is very important for biosensors because it can be identified the specific *E.coli O157:H7* ssDNA target among different kinds of DNA sequences. Curves 1 and 2 show the variation of I-V for *E.coli O157:H7* ssDNA probe and complementary ssDNA target as explained in Figure 2 (C). The non-complementary and single base mismatch targets show a similar trend of I-V as ssDNA probe and $\sim 4.34 \times 10^{-9}$A current is given at 1V as appeared in curve 3and curve 4. It is because non-complementary single base mismatch targets ssDNA cannot bound with immobilized ssDNA probe. They also cannot bind with APTES layer because blocking agents cover the areas which were unreacted with the probe. Hence, non-complementary target ssDNA thoroughly removed after washing with deionized water. Curve 4 shows the same current variation for the single base mismatched target as non-complement.

The concentration dependent detections of target *E.coli O157:H7* were tested electrically by dropping 1µl of different concentrations of targets independently on the active surface on the biosensor. Different concentrations of *E.coli O157:H7* target were prepared from a serial dilution of the 100µM stock. The concentrations of *E. coli* targets, which are 10fM, 10pM, 10nM and 10µM; I-V characteristics were shown in Figure 3 (B). Current at 1V was 5.88×10^{-9}A, 2.04×10^{-8}A, 3.3×10^{-8}A and 4.67×10^{-9}A, respectively as shown in the inset graph of Figure 3 (B). The current values of different concentrations were increased with respect to the increment in the concentration. Thus, different numbers of target ssDNA are hybridized to the same amount of probe on the surface. Thus, the number of proton density on the solid state polymer layer increases and current values are increased proportionally with ssDNA target concentrations.

IV. CONCLUSION

In this research work, we described an electrical AuIDE biosensor on the Si substrate with a novel ssDNA controllable variable resistor through [APTES; $NH_2-(CH_2)_3-Si(OC_2H_5)_3$] solid-state conducting polymer layer for the detection of *E.coli O157:H7*. I-V characteristics were performed for different preparation steps of the biosensor such as bare AuIDE, silanization with APTES and immobilization with synthetic *E.coli O157:H7* target ssDNA. Blocking step with tween-20 was important to detect target specifically. Different current variations indicate for different concentrations of *E. coli* target and it is confirmed that this biosensor is suitable for detect *E.coli O157:H7* target ssDNA

from 10fM to 10µM successfully. The conception mechanism of this biosensor is showing a high-performance to be beneficial for the biosensor industry.

ACKNOWLEDGMENT

REFERENCES

[1] K. Zaid and J. Hh, "Journal of Community Health 2011: Vol 17 Number1 ORIGINAL ARTICLE," J. Community Health, vol. 17, no. 1, pp. 64–73, 2011.

[2] V. Velusamy, K. Arshak, O. Korostynska, K. Oliwa, and C. Adley, "An overview of foodborne pathogen detection: In the perspective of biosensors," Biotechnol. Adv., vol. 28, no. 2, pp. 232–254, 2010.

[3] M. E. Ali, S. Mustafa, U. Hashim, Y. B. Che Man, and K. L. Foo, "Nanobioprobe for the determination of pork adulteration in burger formulations," J. Nanomater., vol. 2012, 2012.

[4] Y. Wang, Z. Ye, C. Si, and Y. Ying, "Subtractive inhibition assay for the detection of E. coli O157:H7 using surface plasmon resonance," Sensors, vol. 11, no. 3, pp. 2728–2739, 2011.

[5] E. De Boer and R. R. Beumer, "Methodology for detection and typing of foodborne microorganisms," Int. J. Food Microbiol., vol. 50, no. 1–2, pp. 119–130, 1999.

[6] K. S. Gracias and J. L. McKillip, "A review of conventional detection and enumeration methods for pathogenic bacteria in food.," Can. J. Microbiol., vol. 50, no. 11, pp. 883–890, 2004.

[7] R. D. A. A. Rajapaksha, U. Hashim, and C. A. N. Fernando, "Design, fabrication and characterization of 1.0 µm Gap Al based interdigitated electrode for biosensors," Microsyst. Technol., 2017.

[8] R. Adzhri et al., "High-performance integrated field-effect transistor-based sensors," Anal. Chim. Acta, vol. 917, pp. 1–18, 2016.

[9] R. D. A. A. Rajapaksha, U. Hashim, M. N. Afnan Uda, C. A. N. Fernando, and S. N. T. De Silva, "Target ssDNA detection of E.coli O157:H7 through electrical based DNA biosensor," Microsyst. Technol., 2017.

[10] M. E. Ali, M. Kashif, K. Uddin, U. Hashim, S. Mustafa, and Y. Bin Che Man, "Species Authentication Methods in Foods and Feeds: The Present, Past, and Future of Halal Forensics," Food Anal. Methods, vol. 5, no. 5, pp. 935–955, 2012.

[11] H. Lin, C. P. Huang, W. Li, C. Ni, S. I. Shah, and Y. H. Tseng, "Size dependency of nanocrystalline TiO2 on its optical property and photocatalytic reactivity exemplified by 2-chlorophenol," Appl. Catal. B Environ., vol. 68, no. 1–2, pp. 1–11, 2006.

[12] N. Wetchakun, B. Incessungvorn, K. Wetchakun, and S. Phanichphant, "Influence of calcination temperature on anatase to rutile phase transformation in TiO2 nanoparticles synthesized by the modified sol–gel method," Mater. Lett., vol. 82, pp. 195–198, 2012.

[13] S.-F. Wang, Y.-F. Hsu, R.-L. Lee, and Y.-S. Lee, "Microstructural evolution and phase development of Nb and Y doped TiO2 films prepared by RF magnetron sputtering," Appl. Surf. Sci., vol. 229, no. 1–4, pp. 140–147, 2004.

[14] S.-H. Song, X. Wang, and P. Xiao, "Effect of microstructural features on the electrical properties of TiO2," Mater. Sci. Eng. B, vol. 94, no. 1, pp. 40–47, 2002.

[15] Y. Wen et al., "A graphene-based fluorescent nanoprobe for silver(i) ions detection by using graphene oxide and a silver-specific oligonucleotide," Chem. Commun., vol. 46, no. 15, p. 2596, 2010.

[16] M. M. N. Nuzaihan et al., "Electrical detection of dengue virus (DENV) DNA oligomer using silicon nanowire biosensor with novel molecular gate control," Biosens. Bioelectron., vol. 83, pp. 106–114, 2016.

[17] T. Adam and U. Hashim, "Highly sensitive silicon nanowire biosensor with novel liquid gate control for detection of specific single-stranded DNA molecules," Biosens. Bioelectron., vol. 67, pp. 656–661, 2015.

[18] S. Nadzirah, N. Azizah, U. Hashim, S. C. B. Gopinath, and M. Kashif, "Titanium dioxide nanoparticle-based interdigitated electrodes: A novel current to voltage DNA biosensor recognizes E. coli O157:H7," PLoS One, vol. 10, no. 10, pp. 1–15, 2015.